INFECTION AND IMMUNITY, Jan. 2002, p. 389–394 Vol. 70, No. 1
0019-9567/02/$04.00+0 DOI: 10.1128/IAI.70.1.389–394.2002

NOTES

Visualization of *Proteus mirabilis* within the Matrix of Urease-Induced Bladder Stones during Experimental Urinary Tract Infection

Xin Li,[1] Hui Zhao,[1]† C. Virginia Lockatell,[2] Cinthia B. Drachenberg,[3] David E. Johnson,[2,4] and Harry L. T. Mobley[1]*

Department of Microbiology and Immunology,[1] Division of Infectious Diseases, Department of Medicine,[2] and Department of Pathology,[3] University of Maryland School of Medicine, and Veterans Affairs Medical Center,[4] Baltimore, Maryland 21201

Received 2 July 2001/Returned for modification 4 September 2001/Accepted 4 October 2001

The virulence of a urease-negative mutant of uropathogenic *Proteus mirabilis* and its wild-type parent strain was assessed by using a CBA mouse model of catheterized urinary tract infection. Overall, catheterized mice were significantly more susceptible than uncatheterized mice to infection by wild-type *P. mirabilis*. At a high inoculum, the urease-negative mutant successfully colonized bladders of catheterized mice but did not cause urolithiasis and was still severely attenuated in its ability to ascend to kidneys. Using confocal laser scanning microscopy and scanning electron microscopy, we demonstrated the presence of *P. mirabilis* within the urease-induced stone matrix. Alizarin red S staining was used to detect calcium-containing deposits in bladder and kidney tissues of *P. mirabilis*-infected mice.

Proteus mirabilis, a gram-negative rod-shaped species in the *Enterobacteriaceae*, is a common cause of urinary tract infection in individuals with long-term urinary catheters in place or individuals with complicated urinary tracts (24, 27). The organism causes a significant bacteriuria, infecting the bladder, but also has a propensity for the kidneys, as demonstrated by bladder washout localization studies (4, 15). *Proteus* infections are perhaps most noted for their association with formation of debilitating kidney and bladder stones (2, 9). In individuals with catheters in place, the catheters often become encrusted with mineral deposits and the lumina become obstructed with crystals, which block the flow of urine (16, 19, 25). In an individual with a complicated urinary tract in which there is a structural abnormality that prevents the normal flow or elimination of urine, stones can form in the lumen of the bladder or within the calices of the kidneys (1). The stones in the kidneys must often be removed surgically or by shockwave lithotripsy (6, 23). *P. mirabilis*, despite its antibiotic sensitivity, can be difficult to clear by antibiotic treatment. It has been hypothesized that bacteria within a stone matrix are protected from antibiotic treatment.

Stones are formed due to the action of the cytoplasmic nickel metalloenzyme urease (7, 19). This enzyme hydrolyzes urea, which is present in urine at concentrations of 0.4 to 0.5 M, generating ammonia and carbon dioxide. Ammonia raises the pH, and normally soluble ions precipitate to form stones, usually composed of magnesium ammonium phosphate (struvite) and calcium phosphate (apatite) (6). Genes involved in urease production in *P. mirabilis* reside on a 6.5-kb DNA fragment that has been cloned and sequenced in our laboratory previously (14). UreR induces transcription of the urease operon, which includes genes encoding the structural subunits, *ureABC*, and genes required for incorporation of Ni^{2+} into the apoenzyme, *ureDEFG* (17, 18).

Previously, was constructed an isogenic urease-negative mutant from *P. mirabilis* wild-type strain HI4320 by disrupting *ureC* through homologous recombination (13). Virulence studies with the murine model of ascending urinary tract infection showed that this urease-negative mutant is severely attenuated in its ability to colonize and persist in bladders and kidneys (12). More importantly, no bladder stone (urolithiasis) or death was observed in any mouse challenged with the urease-negative mutant. In this study, the urease-negative mutant was further characterized and examined by using a CBA mouse model of ascending urinary tract infection involving a long-term indwelling catheter. The presence of bacteria in the stone matrix was investigated by using (i) green fluorescent protein (GFP)-expressing *P. mirabilis* and confocal laser scanning microscopy and (ii) scanning electron microscopy. Finally, alizarin red S stain was used to visualize calcium-containing crystal deposits in bladder and kidney tissues.

Assessment of virulence of the urease-negative mutant (*ureC*) of *P. mirabilis* in catheterized mice. Because *P. mirabilis* is a uropathogen commonly associated with long-term-catheterized patients rather than the general population, we examined the urease-negative mutant and its parental strain by using catheterized CBA mice. Surgical implantation of 4-mm-long long-term catheter segments in the bladders of CBA/J mice was performed as described by Johnson et al. (10, 11).

* Corresponding author. Mailing address: Department of Microbiology and Immunology, University of Maryland School of Medicine, 655 W. Baltimore Street, Room 13-009, Baltimore, MD 21201. Phone: (410) 706-0466. Fax: (410) 706-6751. E-mail: hmobley@umaryland.edu.

† Present address: Department of Pediatrics, Stanford University School of Medicine, Stanford, CA 94305.

TABLE 1. Virulence assessment in CBA mouse model of ascending urinary tract infection

Inoculum		Catheter	No. of deaths/ total no.[a]	No. with urolithiasis/ total no.[b]	Bladder		Kidney	
Strain	Dose (CFU/mouse)				Infection[c]	Colonization[d]	Infection[c]	Colonization[d]
Wild type	10^2	No	1/14	0/5	0/5	2.00 ± 0.00	0/10	2.00 ± 0.00
		Yes	0/19	1/10	2/10	3.01 ± 2.14	4/20	2.59 ± 1.29
	10^4	No	0/15	0/5	0/5	2.00 ± 0.00	4/10	2.81 ± 1.12
		Yes	2/27	7/12	11/12	6.44 ± 1.58	18/24	4.97 ± 1.94
	10^6	No	0/14	1/5	1/5	2.97 ± 2.16	3/10	3.04 ± 1.88
		Yes	2/24	8/11	10/11	6.76 ± 1.62	21/22	5.80 ± 1.39
	10^8	No	12/71	15/20	18/20	6.41 ± 1.94	34/40	6.27 ± 2.44
		Yes	5/13	2/4	4/4	6.53 ± 0.70	8/8	6.24 ± 0.94
	10^9	No	33/106	10/31	29/31	6.50 ± 1.83	52/62	5.70 ± 2.30
		Yes	11/45	3/12	12/12	7.32 ± 0.72	24/24	6.68 ± 1.47
ureC mutant	10^9	No	0/40	0/20	12/20	3.94 ± 2.19	17/40	3.34 ± 1.74
		Yes	0/61	0/30	30/30	6.33 ± 1.46	22/60	2.83 ± 1.26

[a] Number of mice that died before 7 days after challenge/total number of mice.
[b] Number of mice with macroscopically visible bladder stones/total number of mice that survived and were sacrificed on day 7. Statistical differences between groups are indicated in the text.
[c] Number of samples with detectable levels of colonization/total number of samples.
[d] The data are expressed in $\log_{10}$ CFU per gram of tissue and are means ± standard deviations. The level for samples with undetectable colonization was defined as 2 $\log_{10}$ CFU/g of tissue. Statistical differences between groups are indicated in the text.

Two weeks after surgery, the bladders were histologically normal and the mice were transurethrally challenged with either the urease-negative mutant or the wild-type strain. For a comparison of the catheterized model with an uncatheterized model, *P. mirabilis* wild-type strain HI4320 was used to challenge both catheterized and uncatheterized mice at doses of 10^2, 10^4, 10^6, 10^8, and 10^9 CFU/mouse. Seven days after challenge, the mice were sacrificed, and bacteria in the urine, bladders, and kidneys were quantitatively cultured as previously described (12). As shown in Table 1, the catheterized mice were more susceptible than the uncatheterized mice to ascending urinary tract infection by the wild-type *P. mirabilis* strain. At doses of 10^4 and 10^6 CFU/mouse, *P. mirabilis* wild-type strain HI4320 colonized the catheterized mice at significantly higher levels than it colonized the uncatheterized mice; the levels in the bladder were >5,000-fold greater, and the levels in the kidney were >100-fold greater ($P < 0.007$, as determined by the Mann-Whitney test). Increased colonization in the bladder also led to a higher incidence of urolithiasis. At a dose of 10^4 CFU/mouse, 7 of 12 catheterized mice developed urilithiasis, compared with none of the five uncatheterized mice examined ($P = 0.04$, as determined by the Fisher exact test); at a dose of 10^6 CFU/mouse, 8 of 11 catheterized mice developed urolithiasis, compared with one of five uncatheterized mice ($P = 0.08$, as determined by the Fisher exact test).

When challenged with the urease-negative mutant at a dose of 10^9 CFU/mouse, the catheterized mice were more susceptible than the uncatheterized mice to bladder colonization but not to kidney colonization (Table 1). The level of bladder colonization by the urease-negative mutant was >200-fold higher in the catheterized mice than in the uncatheterized mice ($P = 0.0002$, as determined by the Mann-Whitney test). Despite the successful colonization of the bladders of the catheterized mice by the urease-negative mutant, urolithiasis or death was never observed. Although we have shown previously that the urease-negative mutant is severely attenuated in its ability to colonize the urinary tract or cause urolithiasis in uncatheterized CBA mice, we were unable to attribute the lack of urolithiasis directly to the lack of urease because it could have been due to the absence of infection. In the catheterized mice, the level of colonization of the bladder by the mutant was similar to the level of colonization by the wild-type strain. Even so, no bladder stone was ever detected, demonstrating the direct contribution of urease to stone formation in the bladder. The successful colonization of the bladders of the long-term-catheterized mice by the urease-negative mutant raised some concern about the effectiveness of urease-inhibiting drugs for preventing bladder colonization by *P. mirabilis*. As mentioned above, *P. mirabilis* frequently causes urinary tract infections in long-term-catheterized patients. Urease-inhibiting drugs may be very effective in preventing the infection from ascending to the kidneys and eliminating urolithiasis, as indicated by our data. Treatment with such drugs, however, may not completely eradicate bladder colonization by *P. mirabilis* in catheterized patients.

Visualization of GFP-expressing *P. mirabilis* in a bladder stone by confocal laser scanning microscopy. Urease-induced stone formation in patients infected with *P. mirabilis* is detrimental because it often causes persistence and reoccurrence of the infection. It is hypothesized that bacteria within a stone matrix are protected from antibiotic treatment and clearance by the host immune system. To identify the bacteria in a bladder stone, we constructed GFP-expressing *P. mirabilis*. A 760-bp promoterless *gfp*-mut2 (3) was excised from pKEN (generously provided by Brendon Cormack, Johns Hopkins University) by *Xba*I-*Pst*I digestion and cloned into *Xba*I-*Pst*I-digested pBluescript SK (Stratagene, La Jolla, Calif.), resulting in construct pXL7301. *P. mirabilis* HI4320 transformed with pLX7301 constitutively expresses GFP-mut2 from a *lac* promoter on the vector, because *Proteus* species are Lac^-. A bladder stone from an uncatheterized mouse that was challenged with 10^9 CFU of the GFP-expressing *P. mirabilis* and sacrificed on day 4 after challenge was cryogenically fixed, cut into 20-μm sections, and examined with a Carl Zeiss laser scanning microscope (Axiovert 100). Optical planes were scanned with a 488-nm argon laser by using a 515-nm barrier

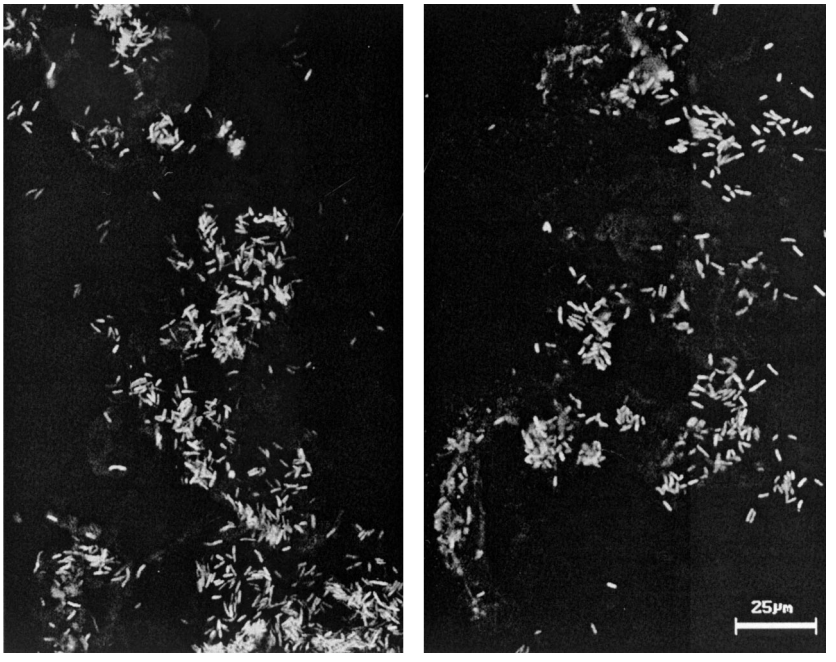

FIG. 1. Confocal images of GFP-expressing *P. mirabilis* in a bladder stone. GFP-expressing *P. mirabilis* in a mouse bladder stone were revealed by confocal laser scanning microscopy. Two representative images are shown. Bar, 25 μm.

filter to detect GFP fluorescence. As shown by two representative micrographs of the stone, abundant GFP-expressing bacteria were present in the bladder stone (Fig. 1).

Visualization of *P. mirabilis* and host immune cells in bladder stones by scanning electron microscopy. Bladders from two uncatheterized mice that developed severe urolithiasis upon experimental urinary tract infection by *P. mirabilis* wild-type strain HI4320 were fixed by instillation of 4% formaldehyde–1% glutaraldehyde for 18 h at room temperature, which kept the bladders in a balloon shape. After fixation, the bladders were sectioned longitudinally in quarters, processed for scanning electron microscopy as described previously (8), and then examined with an AMR model 1000 scanning electron microscope. In most cases of urolithiasis, the bladder stone settles at the inferior end of the bladder, blocking the urethral opening; this was the case for the two bladders analyzed by scanning electron microscopy (Fig. 2A). An infected bladder displayed gross pathological effects, including thickening of the bladder wall and distension of the epithelium. Each bladder stone was compact in its core and had a relatively loose structure in the peripheral layers (Fig. 2B). A significant number of bacteria was not observed on the bladder epithelium or in the core of a bladder stone exposed after sectioning. Most bacteria resided in the loose peripheral layers of the stone (Fig. 2C to E). The surface of the stone was covered with fragments of host cells and an enormous number of bacteria. The majority of the bacteria were short rod-shaped vegetative cells; however, some cells appeared to be elongated swarmer cells.

Bacteria reside within the matrix of bladder and kidney stones in urinary tracts infected with *P. mirabilis*. Using confocal laser scanning microscopy and scanning electron microscopy, we identified bacteria residing within the matrix of stones formed as a result of infection. We observed both short vegetative cells and long swarmer cells in the stone matrix. However, the significance of the presence of the swarmer cells in the stones has not been determined. Is swarmer cell differentiation in a stone merely a surface-induced phenomenon? Do swarmer cells play an active role in the bacterial community living in a stone? Answers to these questions await further investigation. Electron micrographs showed that most bacteria appeared to reside in the peripheral layers of the stone matrix, suggesting that during the development of a stone, bacteria may move out towards the surface of the stone to gain access to nutrients. The deep crevices of the stone may shield bacteria from clearance by host immune cells while allowing access to nutrients. Takeuchi et al. reported the presence of *P. mirabilis* in areas ranging from the nuclei to the peripheral layers in struvite stones (26). Bacteria encased in stones may be protected from antibiotic killing and thus cause persistent or recurrent infections. On the other hand, while the bacteria on the surface have better access to nutrients, they seem to be exposing themselves to killing by antibiotics. It is possible that bacteria living on a stone surface reside in a biofilm and thus are relatively resistant to antibiotic treatment.

Visualization of bladder stones and calcium deposits in kidney tissue with alizarin red S stain. Histochemical staining of bladder stones and calcium deposits in kidney tissue was investigated by using alizarin red S stain. Alizarin red S stain has been used for diagnosis of calcium deposits in tissue (5, 20, 22). Bladder and kidney tissues of uncatheterized mice, infected with wild-type *P. mirabilis*, were fixed in 10% formalin (pH 7.2), embedded in paraffin, and cut into 5- to 7-μm sections. Consecutive sections were stained with a 2% aqueous solution of alizarin red S stain (adjusted to pH 5.6 to 5.8 with 0.1% NH_3) to observe calcium deposits or with hematoxylin and eosin stain to assess the histological damage due to infection.

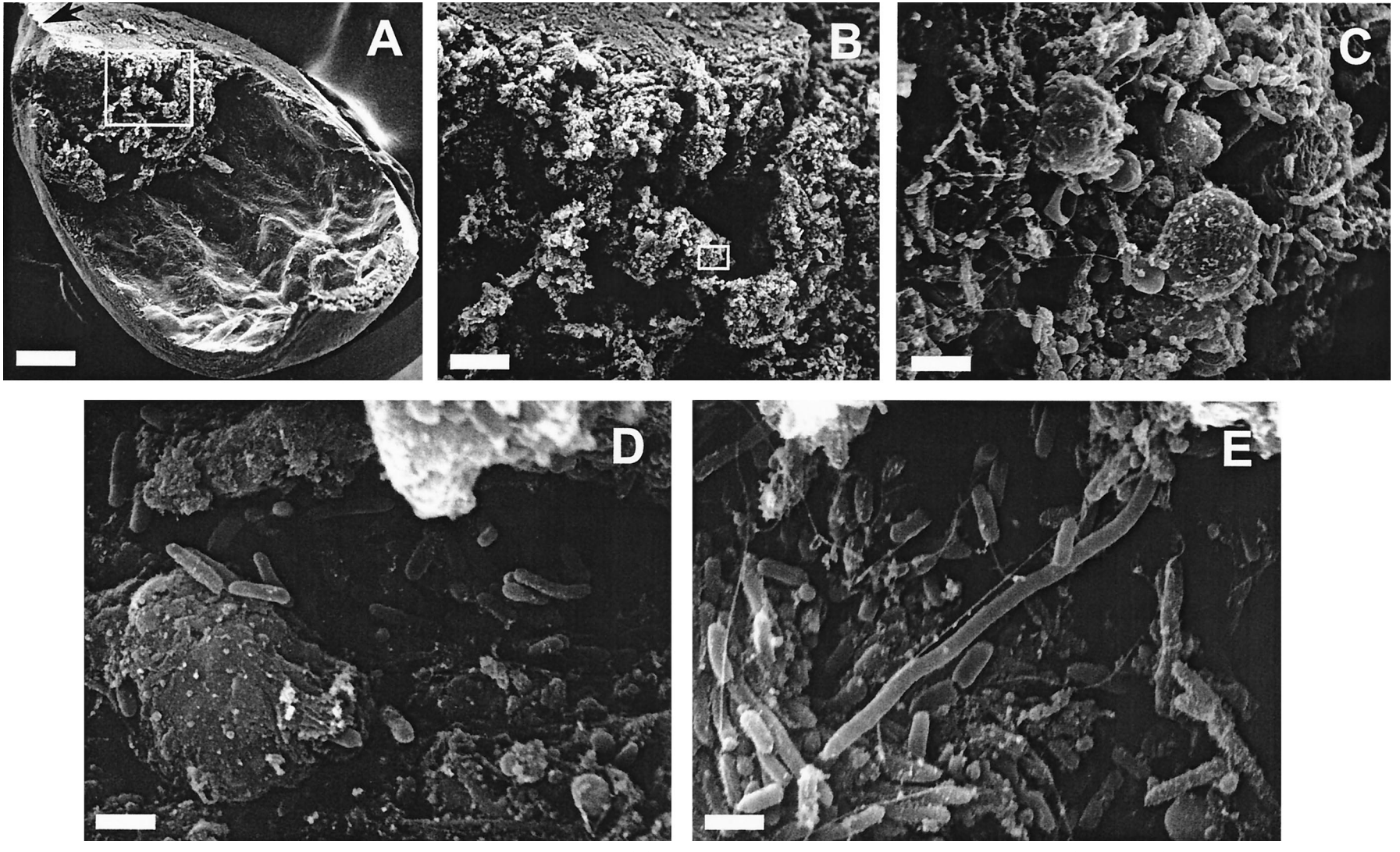

FIG. 2. Scanning electron micrographs of *P. mirabilis* urease-induced bladder stone. (A) One-quarter of the bladder viewed at a low magnification (bar, 500 μm). The orientation of the bladder is indicated by an arrow pointing to the inferior end of the bladder (the end leading to the urethra). (B) Higher magnification (bar, 100 μm) of the area enclosed in a box in panel A. (C) Higher magnification (bar, 5 μm) of the area enclosed in a box in panel B. (D and E) Representative views of the bladder stone (bars, 2 μm).

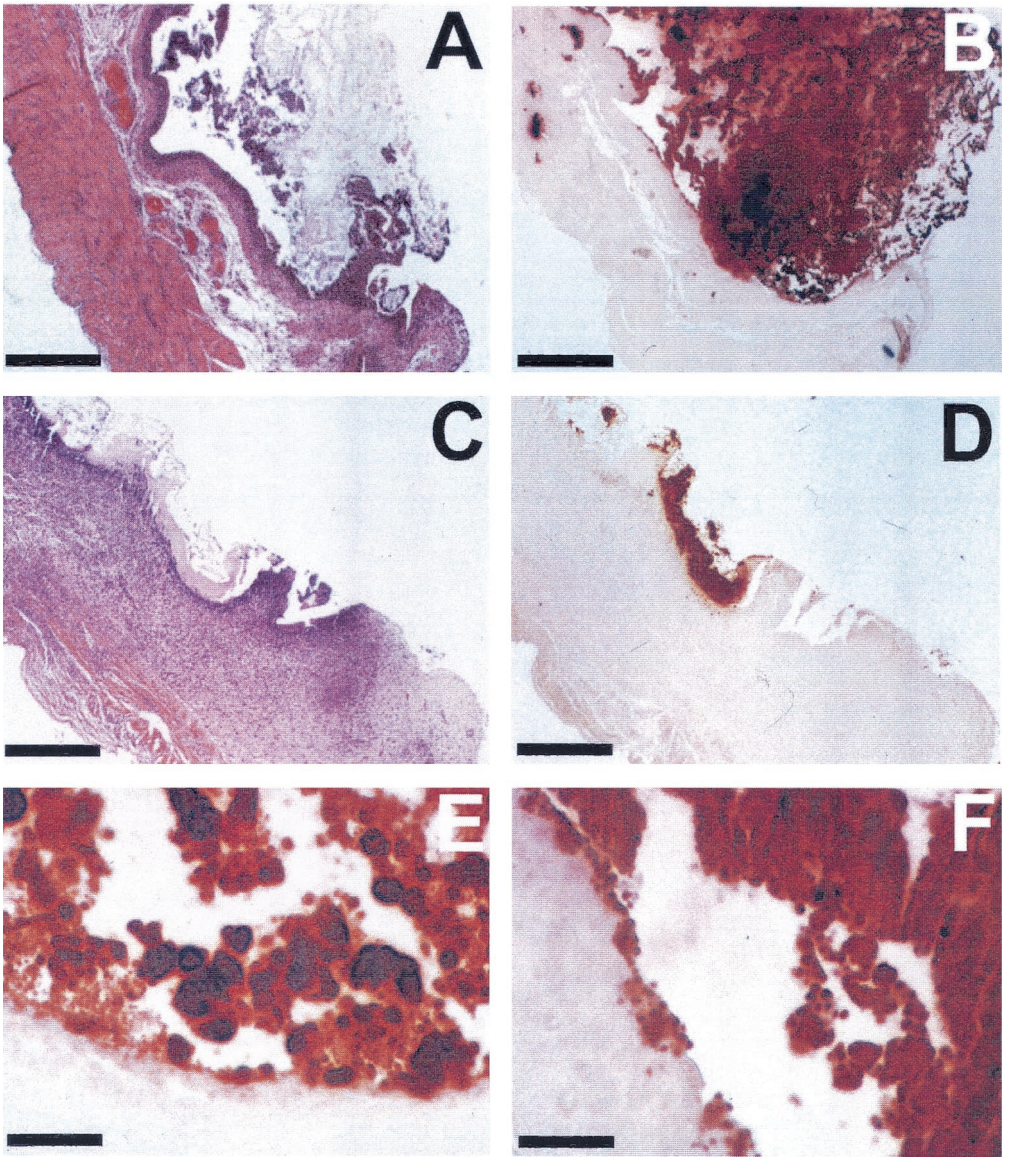

FIG. 3. Sections of *P. mirabilis*-infected mouse bladders stained with hematoxylin and eosin stain and alizarin red S stain. (A and B) Consecutive sections of a mouse bladder that developed a macroscopically visible stone after infection by *P. mirabilis*, stained with hematoxylin and eosin stain and alizarin red S stain, respectively. (C and D) Consecutive sections of a mouse bladder that developed mild urolithiasis due to *P. mirabilis* infection, stained with hematoxylin and eosin stain and alizarin red S stain, respectively. (E and F) Magnified views of areas in panel B, showing mineral deposits on the bladder epithelium stained with alizarin red S stain. Bars, 400 μm for panels A to D and 100 μm for panels E and F.

Samples were examined by light microscopy. As shown in Fig. 3A and B, alizarin red S stained a macroscopically visible bladder stone brick red, creating a drastic contrast to the light pink bladder tissue. Stained mineral deposits were also observed on the bladder epithelium (Fig. 3E and F). Figures 3C and D show a smaller developing bladder stone which was still in close contact with the bladder epithelium. The bladder epithelium in close contact with the stone was strongly stained with hematoxylin, which indicated that severe inflammation and focal necrosis occurred. Similarly, necrotic areas in a kidney with early calcification were stained red with alizarin red S stain (Fig. 4).

Stones appear to form first in association with the surface of necrotic, infected epithelium in both the bladder and the kidney, as revealed by alizarin red S stain. Alizarin red S stain has been used to identify calcium oxalate crystals in the kidneys of patients with familial hyperoxaluria, ethylene glycol poisoning, or chronic renal failure (21, 28). It should be noted that alizarin red S stain is not strictly specific for calcium, and other cations, such as magnesium, manganese, and iron, may interfere with staining. Urease stones are composed of magnesium ammonium phosphate (struvite) and calcium phosphate (apatite) (6). Alizarin red S stain stained bladder stones brick red and stained the tissue very light pink. Using alizarin red S stain, we were able to observe the early stages of bladder stone development, which indicated that stones appear to form first in

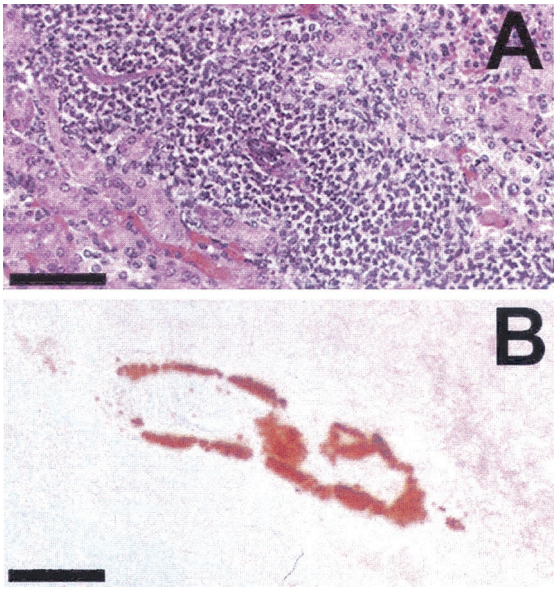

FIG. 4. Sections of *P. mirabilis*-infected mouse kidney stained with hematoxylin and eosin stain (A) and alizarin red S stain (B). A severely necrotic area in the kidney, indicated by the heavy infiltration of host immune cells shown in panel A, was stained with alizarin red S stain, as shown in panel B. Bars, 100 μm.

close association with the bladder epithelium. Alizarin red S staining also revealed calcification of kidney tubules in *P. mirabilis*-infected mice. To correlate alizarin red S staining with infection, we stained consecutive sections of the sample with hematoxylin and eosin stain. In the bladder, alizarin red S-stained calcium deposits correlated well with infection, as indicated by necrosis of the bladder epithelium underneath the stone. In the kidney, however, it was rather difficult to pinpoint the exact location of the calcified tubule in the section stained with hematoxylin and eosin stain due to weak staining of the tissue in the alizarin red S-stained section. Nonetheless, calcification of kidney tubules also correlated well with severe infection in the same area. Further investigation is needed to determine whether the observed calcification of kidney tubules is urease induced.

This work was supported by Public Health Service grants AI23328 and DK47920 from the National Institutes of Health.

We thank Seung H. Chang for technical assistance with scanning electron microscopy.

REFERENCES

1. **Cohen, T. D., and G. M. Preminger.** 1996. Struvite calculi. Semin. Nephrol. **16:**425–434.
2. **Coker, C., C. A. Poore, X. Li, and H. L. T. Mobley.** 2000. Pathogenesis of *Proteus mirabilis* urinary tract infection. Microbes Infect. **2:**1497–1505.
3. **Cormack, B. P., R. H. Valdivia, and S. Falkow.** 1996. FACS-optimized mutants of the green fluorescent protein (GFP). Gene **173:**33–38.
4. **Fairley, K. F., N. E. Carson, R. C. Gutch, P. Leighton, A. D. Grounds, E. C. Laird, P. H. G. McCallum, R. L. Sleeman, and C. M. O'Keefe.** 1971. Site of infection in acute urinary-tract infection in general practice. Lancet **ii:**615–618.
5. **Gilmore, S. K., S. W. Whitson, and D. E. Bowers, Jr.** 1986. A simple method using alizarin red S for the detection of calcium in epoxy resin embedded tissue. Stain Technol. **61:**89–92.
6. **Griffith, D. P.** 1979. Urease stones. Urol. Res. **7:**215–221.
7. **Griffith, D. P., D. M. Musher, and C. Itin.** 1976. Urease: the primary cause of infection-induced urinary stones. Investig. Urol. **13:**346–350.
8. **Gunther, N. W., IV, C. V. Lockatell, D. E. Johnson, and H. L. T. Mobley.** 2001. In vivo dynamics of type 1 fimbria regulation in uropathogenic *Escherichia coli* during experimental urinary tract infection. Infect. Immun. **69:**2838–2846.
9. **Holmgren, K.** 1986. Urinary calculi and urinary tract infection: a clinical and microbiological study. Scand. J. Urol. Nephrol. Suppl. **98:**1–71.
10. **Johnson, D. E., and C. V. Lockatell.** 1999. Mouse model of ascending UTI involving short- and long-term indwelling catheters, p. 441–445. *In* M. Sande (ed.), Handbook of animal models of infection. Academic Press, London, United Kingdom.
11. **Johnson, D. E., C. V. Lockatell, M. Hall-Craigs, and J. W. Warren.** 1991. Mouse models of short- and long-term foreign body in the urinary bladder: analogies to the bladder segment of urinary catheters. Lab. Anim. Sci. **41:**451–455.
12. **Johnson, D. E., R. G. Russell, C. V. Lockatell, J. C. Zulty, J. W. Warren, and H. L. T. Mobley.** 1993. Contribution of *Proteus mirabilis* urease to persistence, urolithiasis, and acute pyelonephritis in a mouse model of ascending urinary tract infection. Infect. Immun. **61:**2748–2754.
13. **Jones, B. D., C. V. Lockatell, D. E. Johnson, J. W. Warren, and H. L. T. Mobley.** 1990. Construction of a urease-negative mutant of *Proteus mirabilis*: analysis of virulence in a mouse model of ascending urinary tract infection. Infect. Immun. **58:**1120–1123.
14. **Jones, B. D., and H. L. T. Mobley.** 1989. *Proteus mirabilis* urease: nucleotide sequence determination and comparison with jack bean urease J. Bacteriol. **171:**6414–6422.
15. **Kohnle, W., E. Vanek, K. Federlin, and H. E. Franz.** 1975. Lokalisation eines Harnwegsinfektes durch Nachweis von antikorperbesetzten Bakterien im Urin. Dtsch. Med. Wochenschr. **100:**2598–2602.
16. **Liedl, B.** 2001. Catheter-associated urinary tract infections. Curr. Opin. Urol. **11:**75–79.
17. **Mobley, H. L. T., and R. P. Hausinger.** 1989. Microbial ureases: significance, regulation, and molecular characterization. Microbiol. Rev. **53:**85–108.
18. **Mobley, H. L. T., M. D. Island, and R. P. Hausinger.** 1995. Molecular biology of microbial ureases. Microbiol. Rev. **59:**451–480.
19. **Mobley, H. L. T., and J. W. Warren.** 1987. Urease-positive bacteriuria and obstruction of long-term urinary catheters. J. Clin. Microbiol. **25:**2216–2217.
20. **Paul, H., A. J. Reginato, and H. R. Schumacher.** 1983. Alizarin red S staining as a screening test to detect calcium compounds in synovial fluid. Anthritis Rheum. **26:**191–200.
21. **Proia, A. D., and N. T. Brinn.** 1985. Identification of calcium oxalate crystals using alizarin red S stain. Arch. Pathol. Lab. Med. **109:**186–189.
22. **Puchtler, H., S. N. Meloan, and M. S. Terry.** 1969. On the history and mechanism of alizarin and alizarin red S stains for calcium. J. Histochem. Cytochem. **17:**110–124.
23. **Rassweiler, J. J., C. Renner, C. Chaussy, and S. Thuroff.** 2001. Treatment of renal stones by extracorporeal shockwave lithotripsy: an update. Eur. Urol. **39:**187–199.
24. **Rubin, R. H., N. E. Tolkoff-Rubin, and R. S. Cotran.** 1986. Urinary tract infection, pyelonephritis, and reflux nephropathy, p. 1085–1141. *In* B. M. Brenner and F. C. Rector (ed.), The kidney. W. B. Saunders Co., Philadelphia, Pa.
25. **Stamm, W. E.** 1991. Catheter-associated urinary tract infections: epidemiology, pathogenesis, and prevention. Am. J. Med. **91:**65S–71S.
26. **Takeuchi, H., H. Takayama, T. Konishi, and T. Tomoyoshi.** 1984. Scanning electron microscopy detects bacteria within infection stones. J. Urol. **132:**67–69.
27. **Warren, J. W., H. H. Tenney, J. M. Hoopes, H. L. Muncie, and W. C. Anthony.** 1982. A prospective microbiologic study of bacteriuria in patients with chronic indwelling urethral catheters. J. Infect. Dis. **146:**719–723.
28. **Yasue, T.** 1969. Histochemical identification of calcium oxalate. Acta Histochem. Cytochem. **2:**83–95.

Editor: D. L. Burns